Magnetic hyperfine interactions in the Zintl phase EuZnSn

Uta Ernet,[a] Ralf Müllmann,[a] Bernd D. Mosel,[a] Hellmut Eckert,[a] Rainer Pöttgen*[,b] and Gunter Kotzyba[b]

[a]*Institut für Physikalische Chemie, Universität Münster, Schlossplatz 4/7, D-48149 Münster, Germany*

[b]*Anorganisch-Chemisches Institut, Universität Münster, Wilhelm-Klemm-Strasse 8, D-48149 Münster, Germany*

Magnetic susceptibility, ^{119}Sn and ^{151}Eu Mössbauer effect measurements are reported for the Zintl phase EuZnSn which crystallizes with the TiNiSi-type structure. The stannide shows Curie–Weiss behaviour above 40 K with an experimental magnetic moment of $\mu_{exp}=7.88(5)\ \mu_B$/Eu, close to that of the free Eu^{2+} ion of $\mu_{eff}=7.94\ \mu_B$. At 20.5(2) K a magnetic phase transition to the antiferromagnetic state is observed in the temperature dependence of the inverse susceptibility at a magnetic flux density of 0.01 T. Magnetization measurements at 5 K indicate metamagnetism with a saturation magnetic moment of $6.80(5)\ \mu_B$/Eu and a critical field of 0.7(1) T. ^{151}Eu Mössbauer measurements show an isomer shift $\delta=-10.9$ mm s^{-1} against EuF_3, as is typically observed for divalent europium. While onset of magnetic ordering is evident at $T_0=26.5(5)$ K, full magnetic order is detected near 15 K. ^{119}Sn Mössbauer spectra show a large transferred magnetic field of 12.8 T at 4.2 K. The temperature dependence of this field is closely correlated with the internal magnetic field measured at the ^{151}Eu site (23.4 T at 4.2 K).

While many structural properties of ternary intermetallic europium compounds have been investigated in recent years,[1,2] little is known about the physical properties of this interesting class of compounds. Magnetic ordering phenomena of such europium compounds can be investigated by complementary susceptibility measurements and ^{151}Eu Mössbauer spectroscopy. The latter technique is also extremely helpful for the determination of the europium valence since the isomer shifts differ significantly, *e.g.* $\delta(EuO)=-11.3$ mm s^{-1} as compared to $\delta(Eu_2O_3)=+1.0$ mm s^{-1}.

Detailed investigations into some physical properties are known only for the EuT_2X_2 (T = transition metal; X = Si, P, Ge) compounds[2] of the large $ThCr_2Si_2$ family[3] and the pnictides EuTX (X = P, As, Sb).[4] We have recently begun a systematic study of the crystal structures and properties of EuTX (X = Si, Ga, Ge, In, Sn)[5–7] compounds. In the present paper we report on the magnetic properties, and the ^{151}Eu and ^{119}Sn Mössbauer spectroscopic characterization of the Zintl phase EuZnSn.[7]

Experimental

A sample of EuZnSn was prepared from the elements in a sealed tantalum tube as described previously.[7] The purity of our sample was checked by a Guinier powder pattern (Cu-Kα_1 radiation) which showed a single-phase material.

The magnetic susceptibilities of a polycrystalline EuZnSn sample were determined with a SQUID magnetometer (MPMS, Quantum Design, Inc.) between 4.2 and 300 K with magnetic flux densities of up to 5.5 T.

^{119}Sn and ^{151}Eu Mössbauer spectroscopic experiments were performed at absorber temperatures between 300 and 4.2 K on a polycrystalline EuZnSn sample from the same batch as for the susceptibility measurements. The $Ca^{119m}SnO_3$ and $^{151}Sm:EuF_3$ sources were held at room temperature. In the case of the ^{119}Sn measurements, a palladium foil of thickness 0.05 mm was used to reduce the tin K X-rays emitted concurrently by the source.

Results and Discussion

Crystal chemistry

The crystal structure of EuZnSn is shown in Fig. 1. EuZnSn adopts the orthorhombic TiNiSi structure, a ternary ordered version of $PbCl_2$. The zinc and tin atoms form puckered Zn_3Sn_3 hexagons which extend in the *yz* plane. While the Zn–Sn intralayer interactions are very strong (Zn–Sn 278 pm), only weak interlayer interactions are observed (Zn–Sn: 305 pm). According to the well known 8-N rule, EuZnSn may be described as a Zintl phase with the formula $Eu^{2+}Zn^{2+}Sn^{4-}$. In emphasizing the essentially covalent character of the zinc–tin intralayer interactions we can also write $Eu^{2+}[ZnSn]^{2-}$. A more detailed description of the EuZnSn structure in comparison with other equiatomic EuTX compounds is given in ref. 7.

Magnetic properties

The temperature dependence of the inverse susceptibility of EuZnSn is plotted in Fig. 2. Above 40 K excellent agreement with the Curie–Weiss law is observed. The experimental magnetic moment, $\mu_{exp}=7.88(5)\ \mu_B$, obtained from the high-temperature slope of the χ^{-1} *vs.* *T* plot according to $\mu_{exp}=2.83\ [\chi\ (T-\Theta)]^{1/2}\ \mu_B$ is very close to the free ion value of $\mu_{eff}=7.94\ \mu_B$ for Eu^{2+} obtained from the relation $\mu_{eff}=g[J(J+1)]^{1/2}\ \mu_B$. The paramagnetic Curie temperature Θ (Weiss constant) of 24(1) K was obtained by extrapolation of the linear χ^{-1} *vs.* *T* plot to $\chi^{-1}=0$. The magnetic behaviour at low temperatures is more complicated. At a magnetic flux density of 0.01 T the inverse susceptibility shows a sharp minimum (inset of Fig. 2) at 20.5(2) K indicating antiferromagnetic ordering. The pronounced minimum has vanished at 2 T. This field-dependent behaviour was investigated in more detail. The magnetization *vs.* external field dependence (Fig. 3) indicates metamagnetism. The transition from antiferromagnetic to ferromagnetic ordering occurs at a critical field (B_C) of 0.7(1) T. At the highest obtainable magnetic flux density of 5.5 T the magnetic

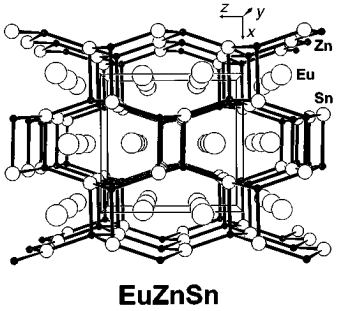

Fig. 1 Perspective view[8] of the crystal structure of EuZnSn along the *y* axis. The polyanion formed by the zinc and tin atoms is outlined.

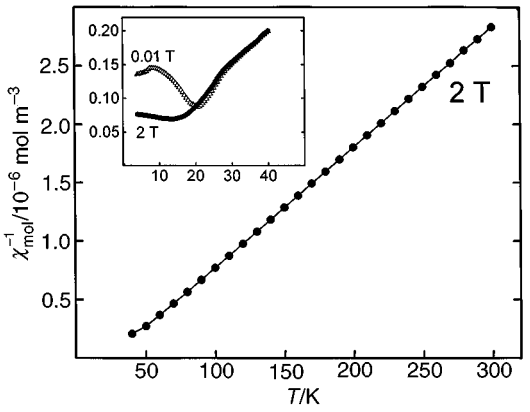

Fig. 2 Temperature dependence of the inverse susceptibility of EuZnSn measured at a magnetic flux density of 2 T. The inset shows the inverse susceptibility at low temperatures measured at 0.01 and 2 T.

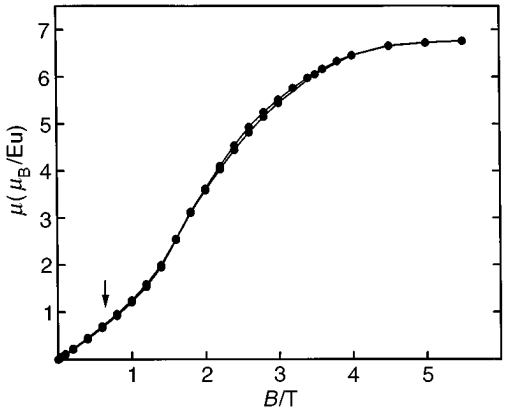

Fig. 3 Magnetization *vs.* external field dependence of EuZnSn at 5 K. The critical field strength is indicated by an arrow.

moment amounts to $\mu_{sm(exp)} = 6.80(5)\ \mu_B$/Eu, very close to the theoretical saturation moment of $\mu_{sm(calc)} = 7.0\ \mu_B$/Eu according to $\mu_{sm(calc)} = gJ\mu_B$. Such metamagnetic behaviour has also been observed recently for the Zintl phases EuZnGe ($\mu_{sm(exp)} = 5.8\ \mu_B$/Eu; $B_C = 0.60$ T),[9] EuCuAs ($\mu_{sm(exp)} = 6.8\ \mu_B$/Eu; $B_C = 0.18$ T)[10] and EuAgAs ($\mu_{sm(exp)} = 6.6\ \mu_B$/Eu; $B_C = 0.25$ T).[10] Note that the values of the critical field are very small for this class of intermetallic compounds, indicating that only small external forces are needed to achieve the rearrangement of the magnetic moments.

Mössbauer spectroscopy

The experimental spectra at 78 K, near the ordering temperature $T_0 = 26.5$ K and at 4.2 K, are shown in Fig. 4 and 5 together with transmission integral fits. Temperature-dependent fit parameters are listed in Tables 1 and 2.

The ^{151}Eu isomer shift of $\delta = -10.9$ mm s^{-1} is typical of divalent europium. An impurity of an unknown Eu^{III} compound can be located at 0.8 mm s^{-1} and is included as a broad Lorentzian (5% in area) in the transmission integral fit at all temperatures. At $T_0 = 26.5(5)$ K magnetic hyperfine splitting is observed. Within the temperature range $26.5 \geqslant T/K \geqslant 18$ the Eu^{II} spectra can be fit to a superposition of a magnetically split component and an unsplit component. The fraction of the latter decreases with temperature, an effect which might be due to a volume distribution of the magnetic particle sizes or to a small degree of disorder within the [ZnSn] polyanion (for more details concerning the order/disorder problems see ref. 6 and 7). As the temperature is decreased the magnetic hyperfine field value increases gradually, reaching a saturation value $B_{sat} = 23.4$ T at 4.2 K. This temperature dependence does not follow the Brillouin function for $J = 7/2$ but is steeper near T_0, which is expected as the Eu–Eu distances $\| y$ are *ca.* 15% larger than $\perp y$. Nevertheless the fit of the 4.2 K spectrum indicates that the electric field gradient, V_{zz}, at the europium site is very small.

In the ^{119}Sn Mössbauer spectra the onset of transferred magnetic hyperfine fields at T_0(Eu) and the superposition with an unsplit fraction is in close correspondence with the magnetic ordering behaviour of Eu^{II}. In accordance with the europium spectra there exists an impurity of another tin compound which is accounted for as a singlet near $\delta = 2.2$ mm s^{-1} at all temperatures. The perfectly symmetric splitting observed at 4.2 K indicates $V_{zz} \approx 0$ and $B_{sat} = 12.8$ T. From Fig. 6 it is obvious that the value of the transferred hyperfine field at the tin site

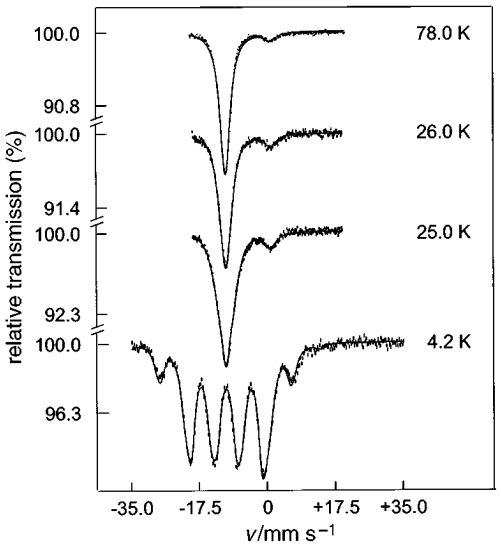

Fig. 4 ^{151}Eu Mössbauer spectra of EuZnSn relative to EuF_3

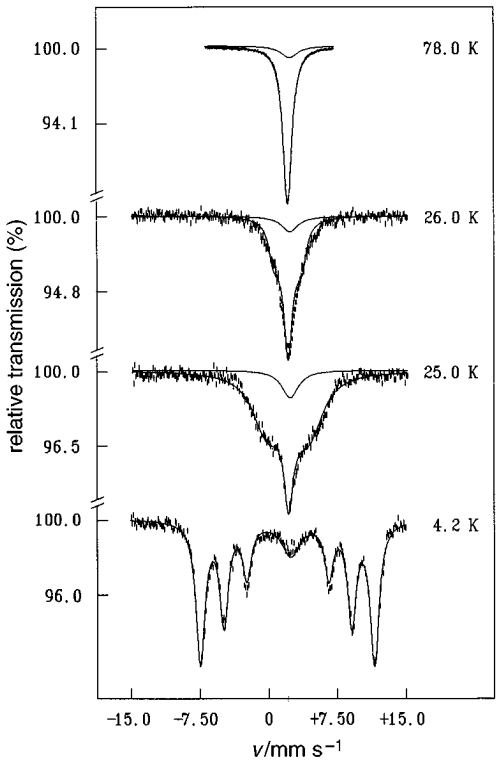

Fig. 5 Experimental and simulated ^{119}Sn Mössbauer spectra of EuZnSn relative to $CaSnO_3$. An impurity component shown separately can be identified at 4.2 K with an isomer shift $\delta = 2.3$ mm s^{-1}.

Table 1 ^{151}Eu Mössbauer fitting parameters for EuZnSn (numbers in parentheses give the statistical errors in the last digit; full width at half height is $W = 2.3$ mm s^{-1} throughout)

T/K	δ^a/mm s^{-1}	$\lvert B_{hf}\rvert^b$/T	$X_{mag}{}^c$
300	−10.88(3)	—	0
78.0	−10.76(1)	—	0
30.0	−10.77(4)	—	0
28.0	−10.76(3)	—	0
26.0	−10.75(3)	2.9(2)	0.6(1)
25.0	−10.75(3)	4.9(2)	0.7(1)
20.4	−10.77(5)	16.9(1)	0.9(1)
15.7	−10.74(6)	21.1(2)	1
11.9	−10.76(5)	21.5(1)	1
4.2	−10.76(5)	23.4(1)	1

[a]Isomer shift. [b]Magnetic flux density. [c]Fraction of europium atoms displaying magnetic hyperfine interactions.

Table 2 ^{119}Sn Mössbauer fitting parameters for EuZnSn (numbers in parentheses give the statistical errors in the last digit; full width at half height is $W = 1.03$ mm s^{-1} with the exception of the value of 25 K, where an artificially large width is probably reflecting a distribution B_{hf})

T/K	δ^a/mms^{-1}	$\lvert B_{hf}\rvert^b$/T	$X_{mag}{}^c$
300	1.91(1)	—	0
78.0	1.94(1)	—	0
30.0	1.98(1)	—	0
27.0	1.97(2)	—	0
26.0	1.98(3)	2.4(1)	0.4(1)
25.0	1.96(3)	3.9(2)	0.8(1)
18.6	1.97(2)	9.4(1)	0.9(1)
13.8	1.97(1)	11.4(1)	1
9.2	1.96(1)	12.4(1)	1
4.2	1.96(2)	12.8(1)	1

[a]Isomer shift. [b]Transferred magnetic flux density. [c]Fraction of tin atoms displaying magnetic hyperfine interactions.

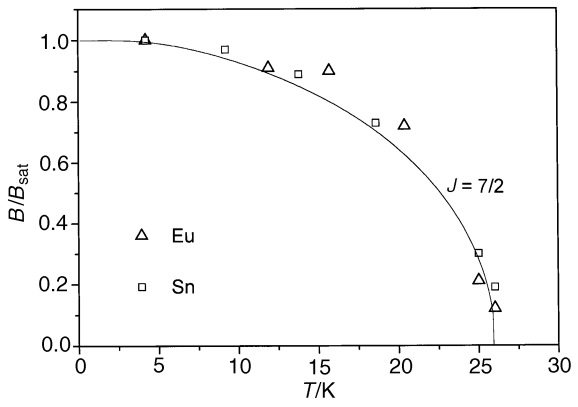

Fig. 6 Temperature dependence of the internal Eu^{II} magnetic hyperfine field and the transferred magnetic field at the tin sites are nearly identical but deviate from the Brillouin function for $J = 7/2$. The values of B_{sat} are 23.4 and 12.8 T for Eu and Sn, respectively.

is proportional to the magnetic field strength at the europium site: $|B_{Sn}(T)| : |B_{Eu}(T)| = |B_{sat,Sn} : B_{sat,Eu}| = 0.55$.

The value of the transferred hyperfine field at the ^{119}Sn site is substantially larger compared to those measured previously in structurally related compounds. For example, $B_{hf} = 8.7$ T has been reported for the binary stannide EuSn with a CrB-type structure.[11] Recently Kruk *et al.*[12] reported ^{119}Sn Mössbauer data for the stannides UTSn (T = Co, Ru, Rh, Ir) which crystallize with the ZrNiAl-type structure (ordered Fe_2P type). These compounds show transferred hyperfine fields between 5.2 and 8.4 T. For the binary antiferromagnetic stannide $MnSn_2$ with crystallographically different tin sites Le Caer *et al.*[13] report transferred fields up to 21 T. Even higher transferred fields (up to 40 T) were measured when the magnetic site of α-MnS is doped with tin.[14]

In other ternary EuTSn (T = Cu, Pd, Pt, Au) compounds magnetic ordering of europium is, with the exception of EuAuSn, also accompanied by transferred magnetic fields at the tin site,[15] but of smaller sizes and with electrical quadrupolar interactions suppressing the complete resolution of the magnetic hyperfine splitting pattern.

G. K. is indebted to Professor Wolfgang Jeitschko for helpful discussions. We are grateful to the Deutsche Forschungsgemeinschaft and the Fonds der Chemischen Industrie for financial support.

References

1 P. Villars and L. D. Calvert, *Pearson's Handbook of Crystallographic Data for Intermetallic Phases*, American Society for Metals, Materials Park, OH, 1991, 2nd edn.
2 A. Szytula and J. Leciejewicz, *Handbook of Crystal Structures and Magnetic Properties of Rare Earth Intermetallics*, CRC Press, Boca Raton, FL, 1994.
3 G. Just and P. Paufler, *J. Alloys Compd.*, 1996, **232,** 1.
4 G. Michels, C. Huhnt, W. Scharbrodt, W. Schlabitz, E. Holland-Moritz, M. M. Abd-Elmeguid, H. Micklitz, D. Johrendt, V. Keimes and A. Mewis, *Z. Phys. B*, 1995, **98,** 75.
5 R. Pöttgen, *J. Mater. Chem.*, 1996, **6,** 63.
6 R. Müllmann, B. D. Mosel, H. Eckert, R. Pöttgen and R. K. Kremer, *Hyperfine Interact.*, in press.
7 R. Pöttgen, *Z. Kristallogr.*, in press.
8 E. Keller, SCHAKAL92, Kristallographisches Institut, Universität Freiburg, 1993.
9 R. Pöttgen, *Z. Kristallogr.*, 1995, **210,** 924.
10 C. Tomuschat and H-U. Schuster, *Z. Anorg. Allg. Chem.*, 1984, **518,** 161.
11 M. Loewenhaupt, *Z. Phys.*, 1974, **267,** 219.
12 R. Kruk, R. Kmiec, K. Latka, K. Tomala, R. Troc and V. H. Tran, *26ièmes Journées des Actinides, Poland, April 10–14, 1996*, Szklarska Poreba, Poland, 1996, P1.5.
13 G. Le Caer, B. Malaman, G. Venturini and I. B. Kim, *Phys. Rev. B: Condens. Matter*, 1982, **26,** 5085.
14 M. Danot, V. E. Tkachenko, K. V. Pokholok, S. Maingaud, P. B. Fabritchny and J. Rouxel, *Mater. Res. Bull.*, 1995, **30,** 563.
15 U. Ernet, R. Müllmann, B. D. Mosel, H. Eckert and R. Pöttgen, unpublished results.

Paper 6/04874I; *Received* 11*th July*, 1996